Carbohydrate Polymers 115 (2015) 276–284

Contents lists available at ScienceDirect

Carbohydrate Polymers

journal homepage: www.elsevier.com/locate/carbpol

Synthesis, characterization and antimicrobial properties of grafted sugarcane bagasse/silver nanocomposites

N.A. Abdelwahab[a,*], N. Shukry[b]

[a] Polymers and Pigments Department, National Research Center, Dokki, Cairo 12311, Egypt
[b] Cellulose and Paper Department, National Research Center, Dokki, Cairo 12311, Egypt

ARTICLE INFO

Article history:
Received 21 April 2014
Received in revised form 19 July 2014
Accepted 22 August 2014
Available online 16 September 2014

Keywords:
Bagasse cellulose
Grafting
Silver nanocomposites
Characterization
Electrical conductivity
Antimicrobial activity

ABSTRACT

Sugarcane bagasse (SCB) was grafted with acrylamide (AAm) and glycidyl methacrylate (GMA) by chemical oxidation method. The effect of monomer/initiator molar ratio, reaction time, reaction temperature and material to liquor ratio on the degree of grafting was investigated. The optimum conditions for grafting were: monomer/initiator molar ratio 1 for AAm and 2 for GMA, reaction time 4 h, reaction temperature 80 °C and materials to liquor ratio 1:20. Silver nanoparticles (AgNPs) were prepared and characterized by X-ray diffraction (XRD) and transmission electron microscopy (TEM). Ungrafted SCB, SCB-g-AAm and SCB-g-GMA were impregnated into silver (Ag) nanoparticles colloidal solution. The ungrafted SCB, grafted SCB and their nanocomposites with Ag nanoparticles were characterized by FT-IR spectroscopy, X-ray diffraction (XRD) and scanning electron microscopy (SEM). The grafted SCB/Ag nanoparticles exhibit better antimicrobial activity against *Escherichia coli* as the model Gram-negative bacteria, *Staphylococcus aureus* as the model Gram-positive bacteria and *Aspergillus flavus* and *Candida albicans* (yeasts) than ungrafted SCB/AgNPs.

1. Introduction

Biopolymers, being renewable raw materials, are gaining considerable importance because of the limited supply of crude oil and the recent environment-conservative regulations (Vineet, Sanjay, & Deepika, 2011). Lignocellulosic natural fibers are characterized by many advantages compared to traditional synthetic fibers. They are eco-friendly, harmless, biodegradable, etc. (Thakur, Thakur, & Gupta, 2013; Singha & Thakur, 2010a). Sugarcane bagasse (SCB), a renewable lignocellulosic resource, is a by-product of the sugar and alcohol industry. It is usually used in pulp and paper industry. However, it is of great importance to explore novel applications of SCB, e.g., in the field of natural fiber composite materials. Cellulose, the main constituent of bagasse (~50%), is embedded in a gel matrix composed of hemicellulose, lignin, and other carbohydrate polymers (Yu, Liu, Shen, Jiang, & Huang, 2005). Cellulosic materials are biodegradable and cannot resist severe environmental conditions due to their hydrophilicity. Therefore, cellulosic materials need to be modified for superior applications (Thakur, Singha, & Thakur, 2012). Many modification processes have been reported in the literature to improve the properties of the natural cellulosic materials (Zhang, Chai, & Fu, 2012). Among these processes graft polymerization has received more attention in the last decade. Grafting of synthetic polymers onto cellulosic materials yields new molecules with desirable properties and having wide range of applications. Varying a set of parameters during synthesis results in materials with precisely tuned properties (Abdel-Halim, 2012; Abdel-Halim & Al-Deyab, 2011b; Hebeish, El-Rafie, Abdel-Mohdy, Abdel-Halim, &Emam, 2010).

Grafting leads to the introduction of special functional groups into cellulose based materials to combine the advantageous properties of cellulose with those of synthetic polymers (Gilles, Erzsébet, László, & Judit, 2011). The grafted polymers are usually synthesized by conventional redox grafting methods (da Silva, de Paula, &Feitosa, 2007), by microwave irradiation (Singh, Tiwari, Pandey, & Singh, 2007), by γ-ray irradiation, or by using the electron beam method (Geresh et al., 2004; Wang, Chen, Zhang, & Yu, 2008). Chemical grafting is one of the most effective methods of modifying the structure and properties of biopolymers. Graft copolymerization of natural polysaccharides is becoming an important issue for developing advanced materials with hydrophobic character (Ly et al., 2010; Meshram, Patil, Mhaske, &Thorat, 2009; Zhu, Dong,

* Corresponding author. Tel.: +20 1223488928.
E-mail address: nor_5020@yahoo.com (N.A. Abdelwahab).

http://dx.doi.org/10.1016/j.carbpol.2014.08.052
0144-8617/

Wang, & Wang, 2010; Cunha & Gandini, 2010; Taghizadeh & Mafakhery, 2001).

Antimicrobial materials and surfaces have great importance in several areas including medical devices, drugs, health care products, water purification systems, hospital furniture, textiles, food packaging, and food storage (Kuorwel et al., 2013; Manso, Cacho-Nerin, Becerril, & Nerín, 2013; Hojatollah et al., 2013; Dankovich & Gray, 2011). It has been found that antimicrobial polymer–metallic composites have excellent antimicrobial properties and potential applications in public health care and biomedical field (Sharma, Yngard, & Lin, 2009). Silver ions and silver compounds have been known to have strong antimicrobial activity (Rinaldi et al., 2013; Nocchetti et al., 2013; Fortunati, Latterini, Rinaldi, Kenny, & Armentano, 2011) against nearly 650 types of bacteria and have potential applications in various fields like antibacterial filters, wound dressing materials, etc. Recently, considerable interest has arisen in the use of silver nanoparticles (AgNPs) based on high antimicrobial and biofouling improvement for water disinfection (Zodrow et al., 2009). It is well known that silver nanoparticles are inert with polymer surfaces, consequently, several approaches were studied to improve loading of AgNPs onto polymer systems, mainly by using a binder or coupler and surface modification by appropriate monomers containing functional groups which have affinity to AgNPs (Nocchetti et al., 2013).

Antimicrobial polymer–silver nanocomposites including polyester/clay/Ag nanocomposites (Konwar, Karak, & Mandal, 2010), chitosan/Ag nanocomposite films (Rhim, Hong, Park, & Ng, 2006), poly(vinyl alcohol)/Ag nanofibers (Hong, Park, Sul, Youk, & Kang, 2006), and poly(methyl methacrylate)/Ag nanofibers (Kong & Jang, 2008) have been synthesized. There have been few reports in the literature on the fabrication of cellulose–silver nanocomposites (Klemencic, Simoncic, Tomsic, & Orel, 2010; Li et al., 2011; Maria et al., 2009; Pinto et al., 2009; Sureshkumar, Siswanto, & Lee, 2010). Maneerung, Tokura, and Rujiravanit (2008) found that impregnating silver nanoparticles into bacterial cellulose led to the formation of nanocomposite with a strong antibacterial activity suitable for antimicrobial wound dressing. Vegetable and bacterial cellulose/Ag nanocomposites with antibacterial activity against Bacillus subtilis, *Staphylococcus aureus* and *Klebsiella pneumoniae* were also studied by Pinto et al. (2009). Moreover, bacterial cellulose/colloidal silver nanocomposites were fabricated using different reductants (hydrazine, hydroxylamine or ascorbic acid) together with gelatin or polyvinylpyrrolidone (Maria et al., 2009). Also, the synthesis of cellulose–silver nanocomposites using ascorbic acid in *N*,*N*-dimethylacetamide as reducing agent has been reported (Li et al., 2011). Recently, magnetic antimicrobial cellulose/silver nanocomposite has been synthesized by a high speed blender using polydopamine as reducing reagent (Sureshkumar et al., 2010).

To the best of our knowledge, no work has been directed towards grafting of acrylamide and glycidyl methacrylate onto sugarcane bagasse. With the target that grafted sugarcane bagasse may find other applications, graft copolymerization of acrylamide and glycidyl methacrylate onto bagasse has been investigated. The reaction conditions for graft copolymerization have been optimized. The ungrafted and grafted bagasse was then loaded with silver nanoparticles (AgNPs) by impregnation of the polymer in AgNPs solution. The ungrafted SCB, grafted products and their Ag nanocomposites were characterized by, FT-IR and SEM. The inhibition zone experiments were carried out to evaluate the antimicrobial activity of ungrafted and grafted sugarcane bagasse/silver nanocomposites against *Escherichia coli (Gram-negative), Staphylococcus aureus* (Gram-positive) bacteria, and *Aspergillus flavus* and *Candida albicans* (yeasts).

2. Experimental

2.1. Materials

Sugarcane bagasse was kindly supplied by a local pulp & paper factory in Quena, Egypt. It was well washed, dried in sunlight and ground into fine particles by centrifugal ball mill of type Fresch, Germany. Acrylamide (AAm) and potassium persulphate (PPS) were supplied by Merck Corporation and were used without purification. Glycidyl methacrylate (GMA), silver nitrate, hydrazine monohydrate, poly(*N*-vinyl pyrrolidone) and ammonium hydroxide were purchased from Aldrich. Solvents used in this work are of analytical grade.

2.2. Preparation of sugarcane bagasse graft copolymers

Grafted bagasse copolymers were synthesized by using potassium persulphate (PPS) as initiator. In order to reduce homopolymer formation, the potassium persulphate was added firstly to bagasse.

The grafting reaction was carried out in a three-necked flask provided with nitrogen inlet and thermometer. 1.0 g of bagasse was dispersed in a definite amount of distilled water followed by the addition of a known quantity of the initiator (PPS). The mixture was immersed in a water bath heated to a certain temperature and stirred for 30 min. 0.8 g of the monomer was then added and the system was continuously stirred for a certain time. After that the product was separated by filtration and washed with 30% aqueous methanol to remove the acrylamide homopolymer or with hot water and dimethyl formamide to remove the glycidyl methacrylate homopolymer. Studied was the effect of changing the monomer: initiator molar ratio (0.25–16), reaction temperature (60–90 °C) and time (1–6 h) as well as material: liquor ratio (1:10–1:30) in order to reach the optimum grafting conditions. The percentage of grafting (%*G*) and grafting efficiency (%*E*) were calculated as follows (Jordan, Guillermo, and Lucille, 2013):

$$\%G = \frac{W_2 - W_1}{W_1} \times 100$$

$$\%E = \frac{W_2 - W_1}{W_3} \times 100$$

where W_1 is the weight of ungrafted SCB, W_2 is the weight of grafted SCB and W_3 is the weight of monomer (acrylamide or glycidyl methacrylate) taken for grafting.

2.3. Preparation of colloidal AgNPs

Silver nanoparticles (AgNPs) colloidal solution was synthesized by reduction of $AgNO_3$ with hydrazine monohydrate in the presence of poly(*N*-vinyl pyrrolidone) (PVP) as stabilizer and to control the particle growth. Aqueous $AgNO_3$ (0.04 mol) solution was added to 100 ml of 0.5 g PVP in ethanol under stirring. Hydrazine monohydrate solution (0.01 mol) was then added dropwise to $AgNO_3$ solution with vigorous stirring and the pH was adjusted to 8 by ammonium hydroxide. The solution was then heated at 60 °C under vigorous stirring until the colour of solution became yellow.

2.4. Immobilization of AgNPs onto SCB, SCB-g-AAm and SCB-g-GMA

Ungrafted SCB, SCB-g-AAm and SCB-g-GMA samples obtained from the optimum grafting conditions were soaked overnight at room temperature in AgNPs colloidal solution for incorporation of AgNPs into grafted polymer network. The resulting

nanocomposites were then filtered and rinsed with distilled water and dried in an oven at 60 °C for 3 h.

2.5. Characterization of samples

2.5.1. Transmission electron microscopy (TEM)

TEM analysis of the prepared AgNPs was performed using (JEM-2100, JEOL Ltd., Japan), the sample was placed on carbon-coated copper grids with Formvar film. The TEM acceleration voltage was 200 kV.

2.5.2. X-ray diffraction (XRD)

X-ray powder diffraction (XRD) patterns of AgNPs, graft copolymers and the nanocomposites were recorded in the range of $2\theta = 10–90^\circ$ on EMPYREAN diffractometer operating at 45 kV with Cu $K\alpha$ ($\lambda = 1.5405$ A°) radiation.

2.5.3. FT-IR spectroscopy

The change in the chemical structure of cellulose fibers in bagasse as result of graft copolymerization and Ag-nanocomposites synthesis was examined using FT-IR spectroscopy. Known weights of the samples and KBr were pressed into disks and measured on JASCO FTIR-4600. The spectra were recorded in the frequency range 4000–400 cm^{-1}.

2.5.4. Scanning electron microscopy (SEM)

The surface morphology of raw SCB, grafted samples and Ag-nanocomposites was observed by using JEOL JXA-840A Electron Probe Microanalyzer. All samples were gold coated before observation.

2.5.5. Electrical conductivity

The electrical conductivity measurements of dry pressed pellets of ungrafted and grafted sugarcane bagasse/silver nanocomposites powder were carried out at ambient temperature by the four-probe technique using a Keithley Hioki3522-50LCP HITESTER electrometer.

2.6. Antimicrobial activity

The antimicrobial activity of ungrafted and grafted SCB/Ag nanocomposites has been investigated against *E. coli* as the model Gram-negative bacteria and *S. aureus* as the model Gram-positive bacteria and also against *A. flavus* and *C. albicans* (yeasts) by conventional spread-plate method (Jiang, Yu, & Chen, 2005). The microorganisms were incubated on Nutrient Agar medium at 37 °C and kept overnight. 100 μl of diluted cell suspension of tested microorganisms were mixed with tested sample and added to Petri dish, incubated at 37 °C for 24 h. Finally, the agar plates were checked for the diameter of inhibition zones.

2.7. Water absorption capacity (swellability)

Water absorption capacity of SCB, SCB-g-AAm and SCB-g-GMA polymers was carried out at room temperature using distilled water (Jordan et al., 2013). In a glass beaker, 0.1 g of ungrafted or grafted SCB was added to 50 ml distilled water. The contents were well covered and allowed to swell for 24 h. The swollen samples were separated from unabsorbed water by filtration through a 100-mesh sieve aluminum screen and the swollen copolymer was weighed. The water absorbency (Q) was calculated as in the following equation. The test was repeated three times for each sample and the average value was recorded.

$$\%Q = \frac{W_1 - W_0}{W_0} \times 100$$

where W_0 is the weight of the dry material and W_1 is the weight of the swollen material in grams.

3. Results and discussions

3.1. Mechanism of grafting

Cellulose is the prime constituent in sugarcane bagasse. The active C_2, C_3 and C_6—OH groups and C—H sites are susceptible to be modified through free radical graft copolymerization. The mechanism of graft copolymerization of acrylamide and glycidyl methacrylate on the cellulose backbone in the presence of potassium persulphate as initiator includes four stages: radical generation, chain initiation, chain propagation and finally chain termination (Toti & Aminabhavi, 2004; Qunwei et al., 2008). Under heating, the persulphate ion solution is decomposed into sulphate ion radicals ($SO_4^{-\bullet}$, R•) (Thakur et al., 2012; Taghizadeh & Mafakhery, 2001; Qunwei et al., 2008). In the initiation step the persulphate ion radicals combine with cellulose OH groups to form cellulose alkoxy radicals which react with the monomer molecules producing cellulose monomer radicals. Also the sulphate ion radicals turn the monomer molecules into radicals. In the propagation step the monomer molecules polymerize on the cellulose monomer radicals to form macroradicals (graft copolymerization). Finally, the reaction is terminated when radical coupling occurs. Also in this step the monomer radicals interact with each other to form homopolymer. The overall reaction is represented in Scheme 1 (Thakur et al., 2013; Taghizadeh & Mafakhery, 2001) and (Scheme 2).

3.2. Optimization of the graft copolymerization parameters

Heterogeneous graft copolymerization of acrylamide and glycidyl methacrylate onto the cellulose backbone in bagasse was carried out in aqueous solution.

The various reaction parameters including monomer to initiator molar ratio, reaction time, reaction temperature as well as material to liquor ratio have been optimized to obtain maximum graft yield.

Radical generation:

$S_2O_8^{-2} \rightarrow 2SO_4^{\bullet}$

Initiation step:

Cell-OH + $R^{\bullet} \rightarrow$ Cell-$O^{\bullet}$ + RH

Cell-$O^{\bullet}$ + Monomer (M) $\rightarrow$ Cell-O-$M^{\bullet}$

M + $R^{\bullet} \rightarrow M^{\bullet}$ + RH

Propagation step:

Cell-O-$M_n^{\bullet}$ + M $\rightarrow$ Cell-O-$M^{\bullet}_{n+1}$

$M_n^{\bullet}$ + M $\rightarrow M^{\bullet}_{n+1}$

Termination step:

Cell-O-$M_n^{\bullet}$ + Cell-O-$M_n^{\bullet}$ $\rightarrow$ graft copolymer

Cell-O-$M_n^{\bullet}$ + Cell-$O^{\bullet}$ $\rightarrow$ graft copolymer

$M^{\bullet}$ + $M^{\bullet}$ $\rightarrow$ homopolymer

Scheme 1. The grafting mechanism of SCB cellulose.

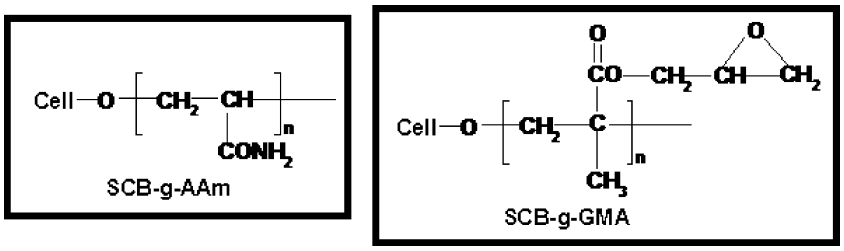

Scheme 2. Chemical structure of SCB-g-AAm and SCB-g-GMA.

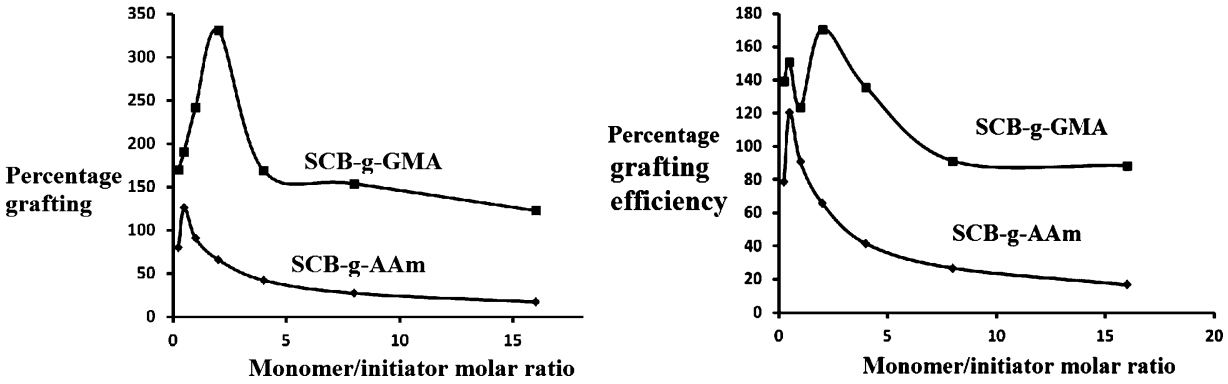

Fig. 1. Effect of monomer/initiator molar ratio upon percentage grafting and percentage grafting efficiency of acrylamide and glycidyl methacrylate onto sugarcane bagasse cellulose (reaction time 3 h, reaction temperature 60 °C and material to liquor ratio 1:20).

3.2.1. Monomer/initiator molar ratio

The monomer/initiator ratio is an important factor that may affect the yield of copolymerization and %*G*. The grafting of acrylamide and glycidyl methacrylate onto sugarcane bagasse has been preliminary investigated at different monomer/initiator molar ratios ranging from 0.25 to 16 and this was carried out under constant temperature (60 °C), time (3 h), and material to liquor ratio (1:20). Fig. 1 shows the effect of various monomer/initiator molar ratios on %*G*, and %*E*. The results indicated that %*G* increased from 80.33 to 125.93% at AAm:initiator ratio 1 and from 170.2 to 330.82% at GMA:initiator ratio 2. Beyond these ratios, a decrease in %*G* has been observed. The initial increase in %*G* may be due to increase in the rate of polymer propagation on the active sites of bagasse cellulose, and the decrease in %*G* can be attributed to lower initiator concentration or monomer depletion which led to a decrease in active sites on the bagasse. GMA showed better results for %*G* and %*E* than AAm as a result of its highly reactive epoxy group (Gilles et al., 2011; Sharma, Kumar, & Soni, 2002; Vismara, melone, Gastoldi, Cosentino& Torri, 2009). The monomer/initiator ratio at maximum %*G* and %*E* is considered optimum and kept constant in further investigations.

3.2.2. Reaction time

Fig. 2 shows the effect of increasing reaction time on percentage grafting and percentage grafting efficiency. %*G* and %*E* were determined at different time intervals ranging from 1 to 6 h under constant monomer/initiator molar ratio (1 for AAm and 2 for GMA), temperature (60 °C) and material to liquor ratio (1:20). From these results, it can be noticed that, the grafting process is positively influenced, in both cases, by increasing the reaction time till 4 h. After that almost no change in %*G* and %*E* could be recognized. The increase in %*G* and %*E* can be attributed to continuous polymer propagation.

3.2.3. Reaction temperature

Fig. 3 illustrates the effect of increasing the reaction temperature from 25 to 90 °C on the graft parameters of both monomers (AAm and GMA). The polymerization reaction was carried out using monomer/initiator ratio 1 for AAm and 2 for GMA for 4 h and material to liquor ratio, 1:20. It has been observed that the percentage grafting and grafting efficiency increased by raising the reaction temperature from 25 to 80 °C and followed by a decrease at 90 °C. It has also been observed that %*G* increased gradually in the case

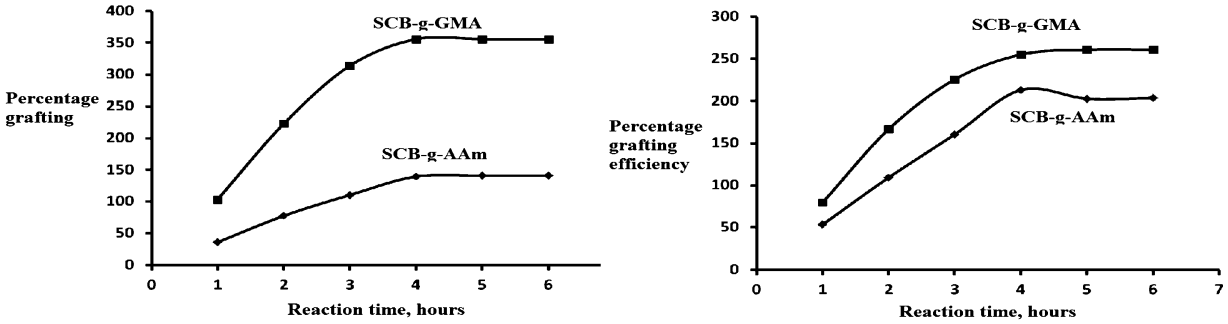

Fig. 2. Effect of reaction time upon percentage grafting and percentage grafting efficiency of acrylamide and glycidyl methacrylate onto sugarcane bagasse cellulose (monomer/initiator molar ratio 1 for SCB-g-AAm and 2 for SCB-g-GMA, reaction temperature 60 °C and material to liquor ratio 1:20).

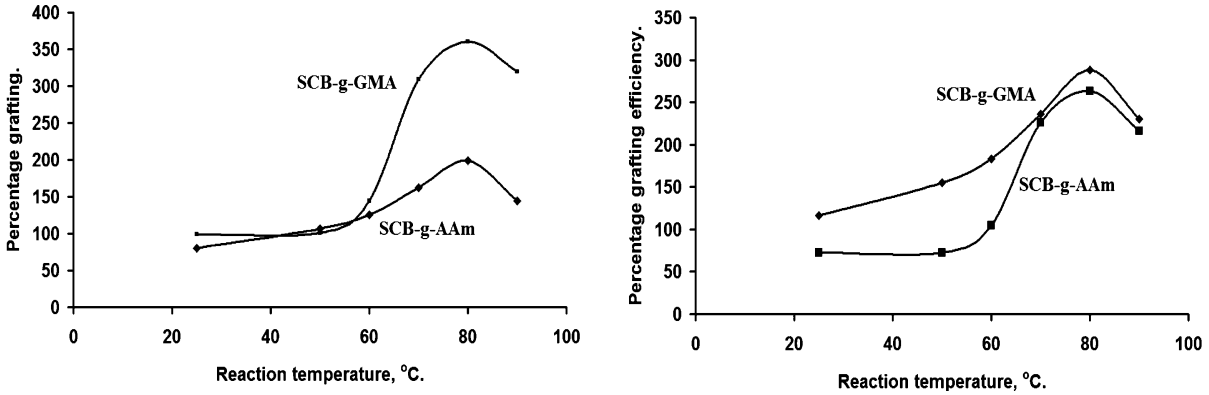

Fig. 3. Effect of reaction temperature upon percentage grafting and percentage grafting efficiency of acrylamide and glycidyl methacrylate onto sugarcane bagasse cellulose (monomer/initiator molar ratio 1 for SCB-g-AAm and 2 for SCB-g-GMA, reaction time 4 h and material to liquor ratio 1:20).

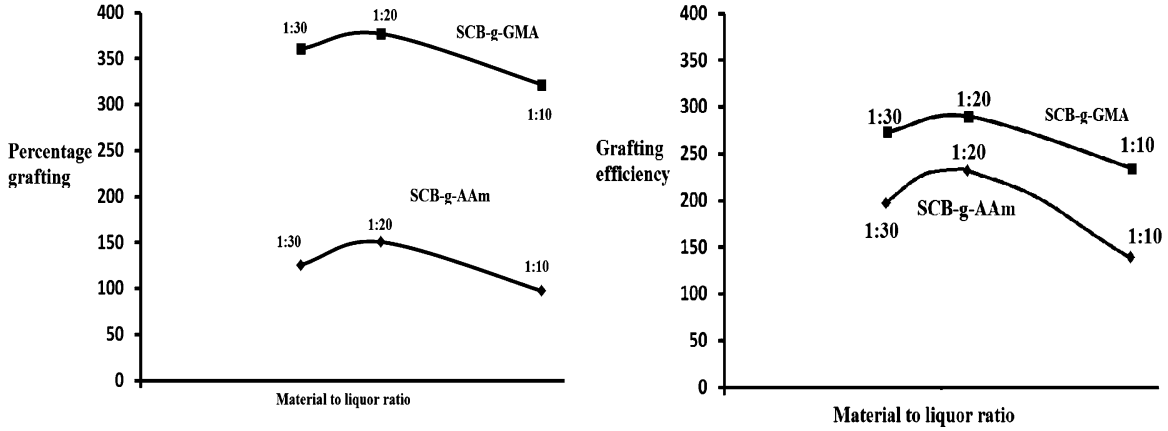

Fig. 4. Effect of material:liquor ratio upon percentage grafting and percentage grafting efficiency of acrylamide and glycidyl methacrylate onto sugarcane bagasse cellulose (monomer/initiator molar ratio 1 for SCB-g-AAm and 2 for SCB-g-GMA, reaction time 4 h and reaction temperature 80 °C).

of AAm, while a steep increase occurred in the case of GMA as the temperature raised from 60 to 80 °C. In general, the high temperature was found to be favorable for graft copolymerization of AAm and GMA onto bagasse cellulose and this can be due to greater molecular collision among reactants, that is monomer and bagasse cellulose macroradicals, so, the rate of initiation and propagation of grafted polymers was accelerated, the rate of initiator decomposition increased and consequently increased the number of free radical sites in the polymerization medium (Toti & Aminabhavi, 2004).

3.2.4. Material to liquor ratio

Fig. 4 shows the effect of changing material to liquor ratio on the percentage grafting and grafting efficiency. It is seen that the graft copolymerization depends also on the ratio of solid reactants to the volume of the polymerization medium. It is suggested that at material:liquor ratio 1:10 the reaction medium possessed higher viscosity and therefore the movability of the reactant molecules and accessibility of bagasse macroradicals decreased. At material to liquor ratio 1:30, the dilution may lead to decrease in molecular collision. The highest percentage grafting and grafting efficiency were achieved at material to liquor ratio 1:20.

3.3. Characterization of grafted copolymers and Ag nanocomposites

3.3.1. TEM

Fig. 5 shows typical TEM image and particle size distribution of silver nanoparticles prepared by reduction of $AgNO_3$ with hydrazine monohydrate in the presence of poly(*N*-vinylpyrrolidone) as stabilizing agent. The nanoparticles are found as dark spherical objects. The size was determined by measuring the diameter of the particles present in the TEM image. The diagram shows wide particle size distribution ranging from 8 nm to 69 nm, i.e., nanoparticles range.

3.3.2. XRD

Fig. 6a–f shows the XRD patterns of AgNPs, SCB/AgNPs, SCB-g-AAm, SCB-g-AAm/AgNPs, SCB-g-GMA and SCB-g-GMA/AgNPs, respectively. AgNPs showed narrow diffraction peaks at $2\theta = 38°$,

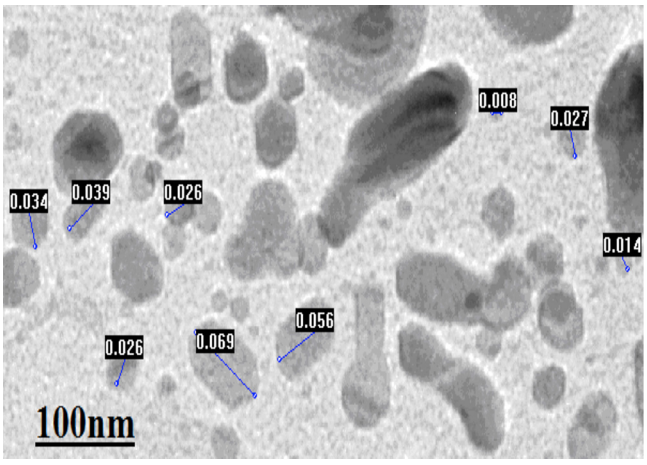

Fig. 5. TEM of AgNPs.

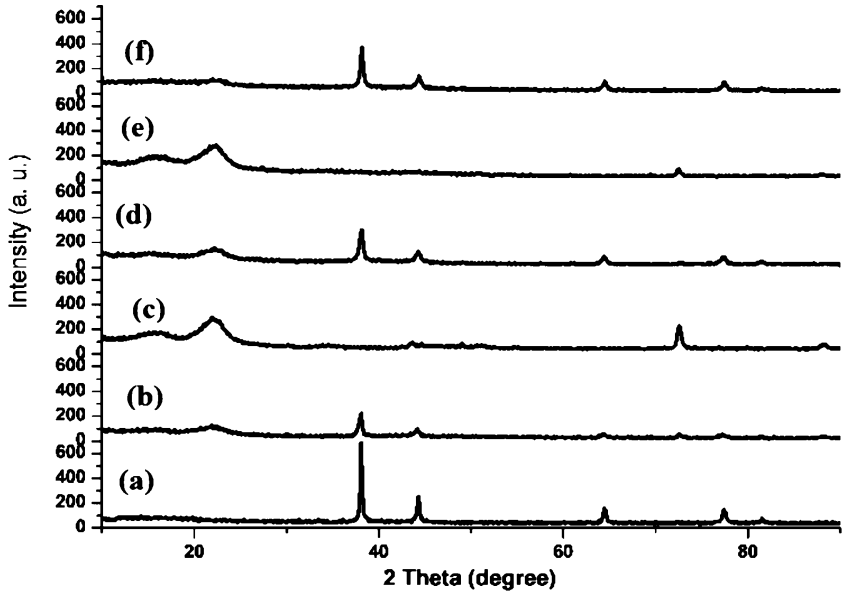

Fig. 6. XRD pattern of (a) AgNPs, (b) SCB/AgNPs, (c) SCB-g-AAm, (d) SCB-g-AAm/AgNPs, (e) SCB-g-GMA and (f) SCB-g-GMA/AgNPs.

44°, 64° and 78°. The same 2θ values were reported by Sharma et al. (2002). Peaks at $2\theta = 16°$, 22° and 72° were observed for SCB-g-AAm and SCB-g-GMA. In XRD patterns of SCB/AgNPs, SCB-g-AAm/AgNPs and SCB-g-GMA/AgNPs nanocomposites additionally the corresponding peaks of AgNPs were detected but with reduced intensity, which confirms the incorporation of AgNPs into SCB and grafted polymers, as well. The intensity of AgNPs peaks is in the following order: SCB-g-GMA/AgNPs > SCB-g-AAm/AgNPs > SCB/AgNPs and this means that grafting increased incorporation of AgNPs and this reflects the positive role of grafting.

3.3.3. FT-IR spectra

The FT-IR spectra of SCB, SCB-g-AAm, SCB-g-GMA, SCB/AgNPs, SCB-g-AAm/AgNPs and SCB-g-GMA/AgNPs samples are represented in Fig. 7a–f. The most characteristic peaks for SCB (Fig. 7a) are: Around 3417 cm^{-1} assigned to OH groups in lignin and carbohydrates, ~2936 cm^{-1} attributed to C—H of lignin and carbohydrates. The band at 1741 cm^{-1} represents the C=O of lignin and xylan and the peaks at 1613 and 1518 cm^{-1} are due to the aromatic ring in lignin while the aromatic C—H occurs at 843 cm^{-1}. The bands at 1386 and 1342 cm^{-1} correspond to C—H. Moreover, the C—O band is observed at 1172 cm^{-1} (Zuqiang et al., 2009). The FT-IR spectra of the copolymers (Fig. 7b and c) showed the bands at 1641 and 904 cm^{-1} corresponding to carbonyl group of acrylamide and epoxy group in glycidyl methacrylate, respectively (Abd-Alla, Mohamed, & Hesham, 2008; Alberti et al., 2005). In general, successful graft copolymerization can be confirmed either by shifts in the frequency or by the change in the intensity of the peaks corresponding to OH and C=O groups. Fig. 7d–f shows FT-IR spectra of SCB/AgNPs, SCB-g-AAm/AgNPs and SCB-g-GMA/AgNPs, respectively. The peaks observed are typically the same as those observed for grafted bagasse but the intensity of OH band increased slightly

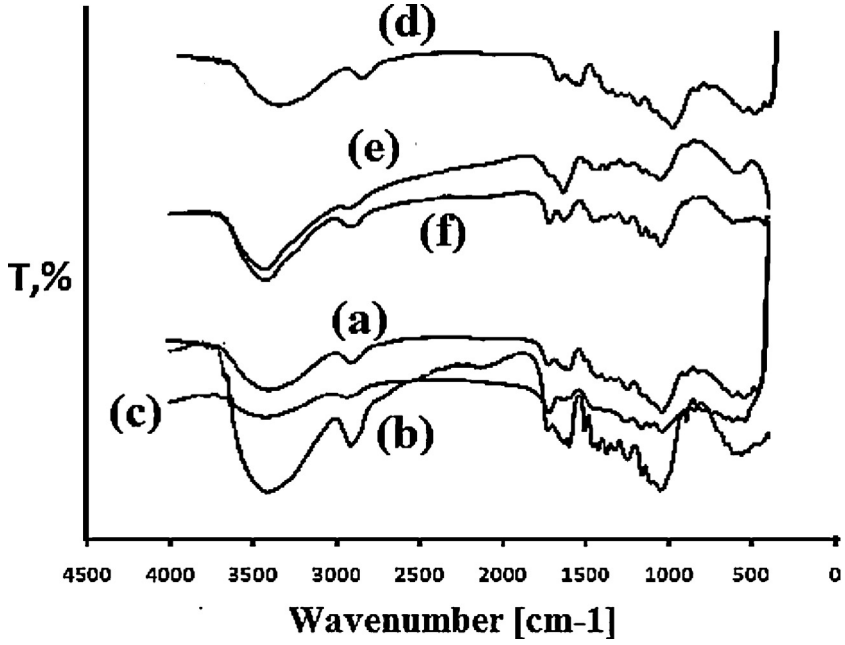

Fig. 7. FT-IR spectra of (a) SCB, (b) SCB-g-AAm, (c) SCB-g-GMA, (d) SCB/AgNPs, (e) SCB-g-AAm/AgNPs and (f) SCB-g-GMA/AgNPs.

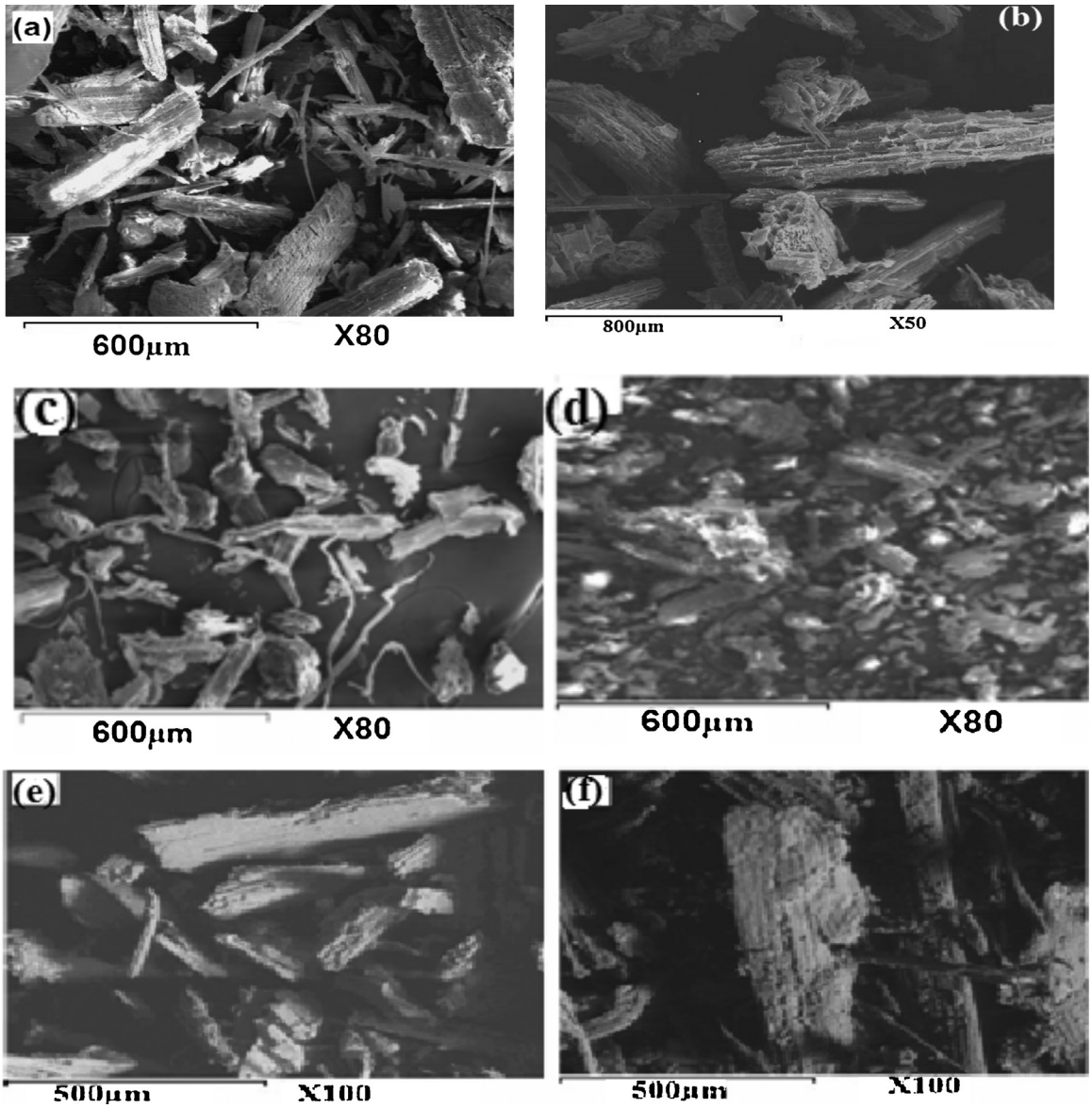

Fig. 8. SEM of (a) SCB, (b) SCB/AgNPs, (c) SCB-g-AAm, (d) SCB-g-GMA, (e) SCB-g-AAm/AgNPs and (f) SCB-g-GMA/AgNPs.

for SCB-g-GMA/AgNPs and decreased for SCB-g-AAm/AgNPs and this may be attributed to incorporation of silver nanoparticles into grafted polymer matrix. The intensity and frequency of the peaks corresponding to SCB and SCB/AgNPs are the same.

3.3.4. Scanning electron microscopy (SEM)

SEM micrographs of SCB, SCB-g-AAm and SCB-g-GMA are shown in Fig. 8a, c, and d. In SCB micrograph (Fig. 8a), the cellulose microfibrils are bound together with lignin and hemicelluloses, where larger fiber bundles with rigid and compact morphology are formed. After grafting, a change in surface morphology was observed and the two samples grafted by the different monomers showed different appearance. SEM image of SCB-g-AAm (Fig. 8c) shows the occurrence of uneven bundles fragmentation upon grafting, but many fibrous structures still exist. In SEM image of SCB-g-GMA (Fig. 8d), a considerable change in the surface morphology is achieved. More disorganized and irregular morphology and smaller fibrous structure are observed. The magnified micrographs (Fig. 8b, e and f) (SCB/AgNPs, SCB-g-AAm/AgNPs and SCB-g-GMA/AgNPs) reveal the irregular and uneven distribution of AgNPs on the fibrous structures and no individual Ag nanoparticles were observed outside the structure. This indicates the strong interaction between the copolymer and Ag nanoparticles. Moreover, in the morphology of the grafted SCB/AgNPs, AgNPs irregularly covered the bundles surface of grafted fibers where in the ungrafted SCB/AgNPs, a poor and disproportionate deposition of AgNPs on the fiber surface appeared.

3.3.5. Electrical conductivity

The results of room temperature a.c. electrical conductivities of ungrafted SCB/AgNPs, SCB-g-AAm/AgNPs and SCB-g-GMA/AgNPs nanocomposites are represented in Table 1. From these results, it is noticed that by increasing the frequency from 50 to 100,000 Hz, the electrical conductivity of the samples increased. SCB-g-AAm/AgNPs and SCB-g-GMA/AgNPs exhibited higher electrical conductivities than ungrafted SCB/AgNPs, the grafting of SCB increased incorporation of AgNPs into the polymer which leads to significant increase in the electrical conductivity. On the other hand, SCB-g-GMA/AgNPs showed higher electrical conductivity values than SCB-g-AAm/AgNPs and this can be attributed to high degree of grafting which increases the opportunity for silver incorporation.

Table 1
Room temperature a.c. electrical conductivity.

Frequency (Hz)	Electrical conductivity (S/cm)		
	SCB/AgNPs	SCB-g-AAm/AgNPs	SCB-g-GMA/AgNPs
50	1.57×10^{-19}	1.7×10^{-16}	1.26×10^{-9}
500	2.66×10^{-15}	2.48×10^{-12}	1.85×10^{-8}
1000	3.86×10^{-13}	4.7×10^{-10}	2.66×10^{-7}
5000	4.92×10^{-11}	5.5×10^{-9}	3.77×10^{-6}
10,000	1.54×10^{-10}	1.65×10^{-7}	5.51×10^{-4}
50,000	2.5×10^{-9}	3.69×10^{-3}	1.33×10^{-3}
100,000	1.9×10^{-7}	1.286	2.05×10^{-1}

Table 2
Antimicrobial activity of ungrafted and grafted SCB and ungrafted and grafted SCB/silver nanocomposites.

Sample	Inhibition zone diameter (mm/mg sample)			
	E. coli	*S. aureus*	*A. flavus*	*C. albicans*
Ungrafted SCB	–	–	–	–
SCB-g-AAm	–	–	–	–
SCB-g-GMA	–	–	–	–
SCB/silver nanocomposites	9	10	–	–
SCB-g-AAm/silver nanocomposites	14	13	–	9
SCB-g-GMA/silver nanocomposites	14	15	9	10

3.4. Antimicrobial activity

The antimicrobial activity of ungrafted SCB, ungrafted SCB/silver nanocomposites, grafted SCB and grafted SCB/silver nanocomposites against *E. coli* as the model Gram-negative bacteria, *S. aureus* as the model Gram-positive bacteria and *A. flavus* and *C. albicans* (yeasts) was measured and the results are represented in Table 2. It has been found that grafted SCB/silver nanocomposites exhibited an inhibition zone while grafted SCB had no effect. However, the ungrafted SCB/silver nanocomposites showed inhibition zone only for the studied bacteria, while it had no effect against the studied yeasts. These results clearly demonstrate that the grafted SCB/silver nanocomposites showed better antimicrobial activity against the studied microorganisms than ungrafted SCB/silver nanocomposites and this confirms that grafting process increased the incorporation of silver nanocomposites and consequently improve the antimicrobial activity. The antimicrobial activity of silver nanoparticles may be attributed to direct damage of cell membranes of microorganisms, the silver nanoparticles can attach to the surface of the cell membrane and thus impair its proper functions, or can penetrate inside the bacteria by diffusion and cause additional cytotoxic and genotoxic effects (AshaRani, Mun, Hande, & Valiyaveettil, 2009). Generally, it has been found that the antibacterial activity against *S. aureus* is higher than that against *E. coli*, for ungrafted SCB/silver nanocomposites and SCB-g-GMA/silver nanocomposites probably due to the difference in cell walls between Gram-negative and Gram-positive bacteria (Heijenoort, 2001). The grafted SCB/Ag nanocomposites also showed antimicrobial activity against *A. flavus* and *C. albicans*, except SCB-g-AAm/AgNPs which had no effect on *A. flavus*. The antimicrobial activity of grafted SCB/silver nanocomposites against bacteria is higher than that against yeasts. Finally, these results clearly confirm that the antimicrobial activity is due to the silver nanoparticles.

3.5. Determination of equilibrium swelling

Equilibrium swelling was calculated as grams of liquid absorbed per gram of dry polymer. Bagasse has relatively low swelling which could be increased or decreased by grafting depending on the type of monomer used in grafting process (Chen, Vassalo, & Chaterjee, 1985). The water absorption test was carried out on the ungrafted and grafted SCB obtained under optimum conditions and the results are listed in Table 3. The increase in water absorbance value for SCB-g-AAm can be due to insertion of hydrophilic parts into the structure of bagasse by grafting, while the drastic decrease in water absorbance value for SCB-g-GMA is explained on the basis of insertion of hydrophobic groups into bagasse structure. It is known that the hydrophobic character is the most commonly desired property of copolymers based on cellulose (Cunha & Gandini, 2010).

Table 3
Water absorbance of ungrafted and grafted bagasse.

Material	Water absorbed (%)
SCB	32.12
SCB-g-AAm	56.54
SCB-g-GMA	12.6

4. Conclusions

SCB-g-AAm and SCB-g-GMA were prepared by polymerization of acrylamide and glycidyl methacrylate onto bagasse cellulose using potassium persulphate as initiator. The study of the factors affecting the polymerization reaction indicated that the optimum conditions for grafting are: monomer/initiator ratio 1 and 2 for AAm and GMA, respectively, reaction time 4 h, reaction temperature 80 °C and material:liquor ratio 1:20. The observation of new bands corresponding to acrylamide and epoxy groups together with some frequency shifts in the FTIR spectra of the copolymers confirms successful grafting and incorporation of AgNPs. Also the incorporation of AgNPs was supported by XRD measurments. New peaks at $2\theta = 38^\circ, 44^\circ, 64^\circ$ and 78° were detected. Change in surface morphology of SCB after grafting was observed in SEM micrographs and grafted SCB/AgNPs composites showed irregular distribution of AgNPs on the fibrous structure. The grafted bagasse/AgNPs nanocomposites showed better antimicrobial activity against *E. coli* and *S. aureus* and also against *A. flavus* and *C. albicans* (yeasts) than ungrafted SCB/AgNPs. From these results it can be concluded that the grafting process improves the incorporation of AgNPs which led to better results corresponding to antimicrobial activity and electrical conductivity results, Moreover, the studied grafted copolymers nanocomposites can be used in many fields of application comprising medical, electrical and disinfection.

Acknowledgment

Financial support for this work was funded by the National Research Center through the project number 10130101. The authors express their deep gratitude to the National Research Center for this support.

References

Abd-Alla, M. A. N., Mohamed, Y. E., & Hesham, M. F. (2008). Synthesis and characterization of grafted cellulose for use in water and metal ions sorption. *BioResources*, *3*, 46–59.
Abdel-Halim, E. S. (2012). Preparation and characterization of poly(acrylic acid)-hydroxyethyl cellulose graft copolymer. *Carbohydrate Polymers*, *90*, 930–936.
Abdel-Halim, E. S., & Al-Deyab, S. S. (2011). Low temperature bleaching of cotton cellulose using peracetic acid. *Carbohydrate Polymers*, *86*, 988–994.
Alberti, A., Bertini, S., Gastaldi, G., Iannaccone, N., Macciantelli, D., Torri, G., et al. (2005). Electron beam irradiated textile cellulose fibres. ESR studies and derivatisation with glycidyl methacrylate (GMA). *European Polymer Journal*, *41*, 1787–1797.
AshaRani, P. V., Mun, G. L. K., Hande, M. P., & Valiyaveettil, S. (2009). Cytotoxicity and genotoxicity of silver nanoparticles in human cells. *ACS Nano*, *3*, 279–290.
Chen, C. C., Vassalo, J. C., & Chaterjee, P. K. (1985). Synthetic and natural polymers. In Chaterjee (Ed.), *Absorbency* (pp. 197–215). The Netherlands: Elsevier Sci. Pub.
Cunha, A. G., & Gandini, A. (2010). Turning polysaccharides into hydrophobic materials: A critical review. *Cellulose*, *17*, 875–889.

da Silva, D. A., de Paula, R. C. M., & Feitosa, J. P. A. (2007). Graft copolymerization of acrylamide onto cashew gum. *European Polymer Journal*, *43*, 2620–2629.
Dankovich, T. A., & Gray, D. G. (2011). Bactericidal paper impregnated with silver nanoparticles for point-of-use water treatment. *Environmental Science and Technology*, *45*, 1992–1998.
Fortunati, E., Latterini, L., Rinaldi, S., Kenny, J. M., & Armentano, I. (2011). PLGA/Ag nanocomposites: In-vitro degradation study and silver ion release. *Journal of Material Science: Materials in Medicine*, *12*, 2735–2744.
Geresh, S., Gdalevsky, G. Y., Gilboa, I., Voorspoels, J., Remon, J. P., & Kost, J. (2004). Bioadhesive grafted starch copolymers as platforms for peroral drug delivery: A study of theophylline release. *Journal of Controlled Release*, *94*, 391–398.
Gilles, D., Erzsébet, T., László, W., & Judit, B. (2011). Cellulose functionalization via high-energy irradiation-initiated grafting of glycidyl methacrylate and cyclodextrin immobilization. *Radiation Physics and Chemistry*, *80*, 1358–1362.
Hebeish, A., El-Rafie, M. H., Abdel-Mohdy, F. A., Abdel-Halim, E. S., & Emam, H. E. (2010). Carboxymethyl cellulose for green synthesis and stabilization of silver nanoparticles. *Carbohydrate Polymers*, *82*, 933–941.
Heijenoort, J. (2001). Formation of the glycan chains in the synthesis of bacterial peptidoglycan. *Glycobiology*, *11*, 25R–36R.
Hojatollah, B. H., Mostofi, Y., Oromiehie, A., Zamani, Z., Ghanbarzadeh, B., Costa, C., et al. (2013). Evaluation of the photocatalytic antimicrobial effects of a TiO_2 nanocomposite food packaging film by in vitro and in vivo tests. *LWT—Food Science and Technology*, *50*, 702–706.
Hong, K. H., Park, J. L., Sul, I. H., Youk, J. H., & Kang, T. J. (2006). Preparation of antimicrobial poly(vinyl alcohol) nanofibers containing silver nanoparticles. *Journal of Polymer Science B: Polymer Physics*, *44*, 2468–2474.
Jiang, S., Yu, W. L., & Chen, H. Y. (2005). Preparation of crosslinked polystyrenes with quaternary ammonium and their antibacterial behavior. *Reactive and Functional Polymers*, *62*, 209–213.
Jordan, F. M., Guillermo, M. N., & Lucille, V. A. (2013). Gamma radiation-induced grafting of glycidyl methacrylate (GMA) onto water hyacinth fibers. *Radiation Physics and Chemistry*, *85*, 182–188.
Klemencic, D., Simoncic, B., Tomsic, B., & Orel, B. (2010). Biodegradation of silver functionalised cellulose fibres. *Carbohydrate Polymers*, *80*, 426–435.
Kong, H., & Jang, J. (2008). Antibacterial properties of novel poly(methyl methacrylate) nanofiber containing silver nanoparticles. *Langmuir*, *24*, 2051–2056.
Konwar, U., Karak, N., & Mandal, M. (2010). Vegetable oil based highly branched polyester/clay silver nanocomposites as antimicrobial surface coating materials. *Progress in Organic Coatings*, *68*, 265–273.
Kuorwel, K., Kuorwel, K. K., Cran, M. J., Sonneveld, K., Miltz, J., & Bigger, S. W. (2013). Migration of antimicrobial agents from starch-based films into a food stimulant. *LWT—Food Science and Technology*, *50*, 432–438.
Li, S. M., Jia, N., Zhu, J. F., Ma, M. G., Xu, F., Wang, B., et al. (2011). Rapid microwave-assisted preparation and characterization of cellulose–silver nanocomposites. *Carbohydrate Polymers*, *83*, 422–429.
Ly, E. B., Bras, J., Sadocco, P., Belgacem, M. N., Dufresne, A., & Thielemans, W. (2010). Surface functionalization of cellulose by grafting oligoether chains. *Materials Chemistry and Physics*, *120*, 438–445.
Maneerung, T., Tokura, S., & Rujiravanit, R. (2008). Impregnation of silver nanoparticles into bacterial cellulose for antimicrobial wound dressing. *Carbohydrate Polymers*, *72*, 43–51.
Manso, S., Cacho-Nerin, F., Becerril, R., & Nerín, C. (2013). Combined analytical and microbiological tools to study the effect on *Aspergillus flavus* of cinnamon essential oil contained in food packaging. *Food Control*, *30*, 370–378.
Maria, L. C. D., Santos, A. L. C., Oliveira, P. C., Barud, H. S., Messaddeq, Y., & Ribeiro, S. J. L. (2009). Synthesis and characterization of silver nanoparticles impregnated into bacterial cellulose. *Materials Letters*, *63*, 797–799.
Meshram, M. W., Patil, V. V., Mhaske, S. T., & Thorat, B. N. (2009). Graft copolymers of starch and its application in textiles. *Carbohydrate Polymers*, *75*, 71–78.
Nocchetti, M., Donnadio, A., Ambrogi, V., Andreani, P., Bastianini, M., Pietrella, D., et al. (2013). Ag/AgCl nanoparticle decorated layered double hydroxides: Synthesis, characterization and antimicrobial properties. *Journal of Material Chemistry B*, *1*, 2383–2393.
Pinto, R. J. B., Marques, P. A. A. P., Neto, C. P., Trindade, T., Daina, S., & Sadocco, P. (2009). Antibacterial activity of nanocomposites of silver and bacterial or vegetable cellulosic fibers. *Acta Biomaterialia*, *5*, 2279–2289.
Qunwei, T., Jihuai, W., Hui, S., Shijun, F., De, H., & Jianming, L. (2008). Superabsorbent conducting hydrogel from poly(acrylamide-aniline) with thermo-sensitivity and release properties. *Carbohydrate Polymers*, *73*, 473–481.
Rhim, J. W., Hong, S. I., Park, H. M., & Ng, P. K. W. (2006). Preparation and characterization of chitosan-based nanocomposite films with antimicrobial activity. *Journal of Agricultural and Food Chemistry*, *54*, 5814–5822.
Rinaldi, S., Fortunati, E., Taddei, M., Kenny, J. M., Armentano, I., & Latterini, L. (2013). Integrated PLGA–Ag nanocomposite systems to control the degradation rate and antibacterial properties. *Journal of Applied Polymer Science*, *130*, 1185–1193.
Sharma, V. K., Yngard, R. A., & Lin, Y. (2009). Silver nanoparticles: Green synthesis and their antimicrobial activities. *Advances in Colloid and Interface Science*, *145*, 83–96.
Sharma, B. R., Kumar, V., & Soni, P. L. (2002). Ceric ammonium nitrate initiated graft copolymerization of acrylamide onto Cassia tora gum. *Journal of Applied Polymer Science*, *86*, 3250–3255.
Singh, V., Tiwari, A., Pandey, S., & Singh, S. K. (2007). Peroxydisulfate initiated synthesis of potato starch-graft-poly(acrylonitrile) under microwave irradiation. *Express Polymer Letters*, *1*, 51–58.
Singha, A. S., & Thakur, V. K. (2010). Synthesis and characterization of short *Grewia optiva* fiber based polymer composites. *Polymer Composites*, *31*, 459–470.
Sureshkumar, M., Siswanto, D. Y., & Lee, C. K. (2010). Magnetic antimicrobial nanocomposite based on bacterial cellulose and silver nanoparticles. *Journal of Materials Chemistry*, *20*, 6948–6955.
Taghizadeh, M. T., & Mafakhery, S. (2001). Kinetics and mechanism of graft polymerization of acrylonitrile onto starch initiated with potassium persulphate. *Sciences Islamic Republic of Iran*, *12*, 333–338.
Thakur, V. K., Singha, A. S., & Thakur, M. K. (2012). Graft copolymerization of methyl acrylate onto cellulosic fibers: Synthesis, characterization and applications. *Journal of Polymers and Environment*, *20*, 164–174.
Thakur, V. K., Thakur, M. K., & Gupta, R. K. (2013). Graft copolymers from cellulose: Synthesis, characterization and evaluation. *Carbohydrate Polymers*, *97*, 18–25.
Toti, U. S., & Aminabhavi, T. M. (2004). Modified guar gum matrix tablet for controlled release of diltiazem hydrochloride. *Journal of Control Release*, *95*, 567–577.
Vineet, K., Sanjay, N., & Deepika, P. (2011). Optimization of reaction conditions for grafting of α-cellulose isolated from *Lantana camara* with acrylamide. *Carbohydrate Polymers*, *86*, 760–768.
Vismara, E., melone, L., Gastoldi, G., Cosentino, C., & Torri, G. (2009). Surface modification of cotton cellulose with glycidyl methacrylate and its application for the adsorption of aromatic pollutants from waste waters. *Journal of Hazardous Materials*, *170*, 798–808.
Wang, J. P., Chen, Y. Z., Zhang, S. J., & Yu, H. Q. (2008). A chitosan-based flocculant prepared with gamma-irradiation-induced grafting. *Bioresource Technology*, *99*, 3397–3402.
Yu, H., Liu, R. G., Shen, D. W., Jiang, Y., & Huang, Y. (2005). Study on morphology and orientation of cellulose in the vascular bundle of wheat straw. *Polymer*, *46*, 5689–5694.
Zhang, J. F., Chai, X. S., & Fu, S. Y. (2012). Homogeneous grafting poly(methyl methacrylate) on cellulose by atom transfer radical polymerization. *Carbohydrate Polymers*, *87*, 1869–1873.
Zhu, J., Dong, X., Wang, X., & Wang, Y. (2010). Preparation and properties of a novel biodegradable ethyl cellulose grafting copolymer with poly(*p*-dioxanone) side chains. *Carbohydrate Polymers*, *80*, 350–359.
Zodrow, K., Brunet, L., Mahendra, S., Li, D., Zhang, A., Li, Q., et al. (2009). Polysulfone ultrafiltration membranes impregnated with silver nanoparticles show improved biofouling resistance and virus removal. *Water Research*, *43*, 715–723.
Zuqiang, H., Xingtang, L., Huayu, H., Li, G., Yongjun, C., & Zhangfa, T. (2009). Influence of mechanical activation on the graft copolymerization of sugarcane bagasse and acrylic acid. *Polymer Degradation and Stability*, *94*, 1737–1745.